Microscopic structure of nanometer-sized silica particles

Uchino, Takashi ; Aboshi, A. ; Kohara, S. ; Ohishi, Y. ; Sakashita, M. ; Aoki, K.

Microscopic structure of nanometer-sized silica particles

T. Uchino,[1,2] A. Aboshi,[1] S. Kohara,[3] Y. Ohishi,[3] M. Sakashita,[4] and K. Aoki[4]
[1]*Department of Chemistry, Kobe University, Nada-ku, Kobe 657-8501, Japan*
[2]*PRESTO, Japan Science and Technology Corporation, Kawaguchi, Saitama 332-0012, Japan*
[3]*SPring-8, Japan Synchrotron Radiation Research Institute, Sayo, Hyogo 679-5198, Japan*
[4]*National Institute of Advanced Industrial Science and Technology, Tsukuba, Ibaraki 305-8565, Japan*
(Received 5 June 2003; revised manuscript received 6 January 2004; published 12 April 2004)

We have studied the structure of nanometer-sized silica particles called fumed silica, which is a synthetic amorphous silicon dioxide produced by burning silicon tetrachloride in an oxygen-hydrogen flame, using infrared and Raman spectroscopies and a high-energy x-ray diffraction method. It has been demonstrated that the structure of fumed silica is not identical to that of the normal bulk silica glass in terms especially of the distribution of the size of silica rings. Three- and four-membered rings are more frequent in fumed silica than in the bulk silica glass. It has also been shown that the network structure of fumed silica is more flexible than that of the bulk one, probably explaining the reason why fumed silica can accommodate a large number of three- and four-membered rings in the structure.

DOI: 10.1103/PhysRevB.69.155409 PACS number(s): 61.43.−j, 61.10.−i

I. INTRODUCTION

Recently, condensed phases with reduced dimensions and size have been shown to exhibit numerous instances in which one bonding geometry appears to be favored over others at a given pressure and/or a temperature.[1–3] One of the most intriguing examples of this behavior can be seen in carbon-based materials, including fullerenes and carbon nanotubes. In contrast to the case of crystalline and/or ordered materials, the size dependence of the structure of amorphous materials has hardly been investigated. This is primarily because the structure of disordered materials is usually not well defined, and the measurements of the size dependence of their structure are often a challenging task.

Although a full knowledge of their structure is still lacking, amorphous small fine particles have attracted considerable attention in recent years. In particular, silica-based nanophase materials have been the subject of recent studies because of their potential applications in nanoscale silicon optoelectronic devices.[4–7] One example of such extremely small silica particles is fumed silica, which is produced at high temperature (1400–1800 °C) by the hydrolysis of silicon tetrachloride vapor in a flame of hydrogen and oxygen. Since fumed silica has very high specific surface area ($\sim 100 - \sim 400\ m^2/g$), its surface reactivity and the related surface properties have been studied by many researchers during the past decades.[8] These properties depend basically on the quantity and structural environment of its surface hydroxyl groups.[9,10] However, structural studies on fumed silica itself have been very limited,[11–13] and the structural difference between fumed silica and the bulk silica glass has not been well recognized.

Recently, molecular dynamics (MD) simulations for silica clusters containing $\sim 10^3$ to $\sim 10^4$ atoms have been reported to understand the structure and properties of nanometer-sized silica particles.[14–16] It has been found that the density distribution function for the silica clusters shows a small peak just below the surface,[15,16] suggesting a shell-like structure or a local chemical ordering near the surface. It has also been found that such small clusters have much higher internal pressures, higher diffusion coefficient of the constituent oxygen and silicon atoms, and lower melting temperature as compared with the corresponding bulk materials.[15,16] The results of these MD computer simulations strongly suggest that the structure of amorphous silica is altered as a function of the particle size, probably rationalizing a size dependence of the related properties.

In contrast to the theoretical approaches, structural studies on nanometer-sized amorphous silica particles such as fumed silica are rather few apart from the studies on their surface hydroxyl groups as mentioned earlier. However, we have recently reported that fumed silica exhibits a unique structural modification under pressure.[17,18] That is, a pressure-induced structural transition, accompanied by densification, occurs at lower pressures (2–8 GPa) than would normally be expected for bulk silica glass (over 10 GPa). This suggests that nanometer-sized silica particles have a lower threshold for irreversible compaction than bulk silica glass. This unprecedented behavior of fumed silica most likely results from the intrinsic structural characteristics of the material, and a detailed knowledge of the structure will be useful for a better understanding of the properties of the fine-particle oxides. In this work, we, therefore, carry out a series of structural analysis of fumed silica using infrared and Raman spectroscopies and a high-energy x-ray diffraction method. We then investigate how the structure of fumed silica is modified after heat treatment and under pressure.

II. EXPERIMENTAL SECTION

This work was carried out by using a nonporous amorphous fumed silica [specific surface area $= 390 \pm 40\ m^2/g$; particle size 7 nm (product specification)] obtained from Sigma. The sample was heated at different temperatures ranging from 900 to 1200 °C for 2 h to remove surface hydroxyl groups, including hydrogen bonded and isolated silanols (≡Si—OH groups which are not hydrogen bonded to each other) or molecular water. According to previous dehy-

droxylation studies on fumed silica,[10,19] little or no evidence of hydrogen-bonded silanols or water molecules is seen when the dehydroxylation temperature reaches 800 °C; the residual isolated silanol concentration for the samples heated at 900 °C is estimated to be ~1 OH/nm^2 (Ref. 10). Thus, it is likely that most of the hydrogen-bonded silanols along with physically adsorbed molecular water are dehydroxylated by this heat treatment although not all the surface OH groups especially in the form of isolated silanols, cannot be removed completely. The Brunauer-Emmett-Teller (BET) specific surface areas of the heat-treated samples were obtained using a conventional volumetric adsorption apparatus with nitrogen adsorption. Changes in the particle morphology with temperature were also characterized by field emission scanning electron microscopy (FESEM) with a JEOL JSM-6700F microscope operating at 1.5 kV.

Fourier transform infrared (FTIR) spectra of the fumed silica samples were recorded with a Perkin-Elmer Spectrum 1000 spectrometer. A conventional KBr disc technique was employed to measure the FTIR spectra in the frequency region associated with the Si—O—Si stretching and bending vibrations, ranging from 400 to 1600 cm^{-1}. We also measured an overtone of the Si—O—Si stretching vibration, which is located at ~2260 cm^{-1} and has been shown to be related to the fictive temperature of silica glass.[20] The fictive temperature of a glass is defined[21] as ''the temperature at which the glass would find itself in equilibrium if suddenly brought to that temperature from its given state.'' It has also been demonstrated that the glass network undergoes steric changes as function of the fictive temperature.[22] It is hence interesting to obtain the fictive temperature of the present samples to get a better knowledge of their microscopic structure. Since the intensity of such an overtone mode is rather weak, the heat-treated fumed silicas were pressed into pellets with ~1 mm thickness, and the FTIR absorption spectra were measured in transmission mode.

Raman spectra were obtained on a Perkin-Elmer System 2000R NIR Fourier-transform Raman (FT-Raman) spectrometer. The laser used in the FT-Raman spectrometer is Nd:YAG (an yttrium aluminum garnet crystal doped with triply ionized neodymium), emitting laser radiation at 1064 nm. We also tried to obtain Raman spectra with a conventional dispersive Raman spectrometer where spectra are collected using an excitation wavelength in the visible range. However, Raman measurements using visible laser radiation caused strong florescence and/or scattering resulting probably from unknown surface defects of fumed silica. This problem was virtually eliminated using FT-Raman spectroscopy that employs a near-infrared (1064 nm) laser for excitation.

We should also note that on removal of the hydroxyl groups at 900–1200 °C, the fumed silica surface would no longer physically absorb water and would not be rehydrated.[23] This indicates that the present heat-treated samples are quite stable even in ambient condition. Indeed, we have confirmed that the infrared and Raman spectra observed for the present heat-treated samples are basically unchanged after exposure to ambient condition for two months.

The structure of fumed silica was also investigated by using high-energy x-ray rays supplied by synchrotron radiation. Since the energy of the incident photons used in the experiments is quite high (61.6 keV), the resulting photoelectrical absorption is significantly decreased.[24] High-energy x-ray diffraction has additional further advantages, e.g., the wide accessible Q range, the small scattering angles and the diminishing correlation terms.[24] These specific characteristics of high-energy x-ray measurements enable us to obtain the sufficiently high resolution in the real-space correlation functions, which can be comparable to those obtained from a typical neutron diffraction experiment. The high-energy x-ray diffraction experiments of the fumed silica samples were performed in transmission geometry using the bending magnet beamline BL04B2 (Ref. 25) at SPring-8, Hyogo, Japan, with a horizontal two-axis diffractometer.[26] In this work, x-ray diffraction data were measured up to $Q_{\max}=25$ Å^{-1} [$Q=(4\pi/\lambda)\sin\theta$] for the dehydroxylated fumed silica samples as well as normal bulk silica glass.

TABLE I. BET surface areas and apparent morphology of fumed silica samples heated at different temperatures.

Heating temperature (°C)	BET surface area (m^2/g)	apparent morphology
as received	390 ± 40[a]	fluffy very fine powder
1000	188	fluffy very fine powder
1100	115	fine powder
1200	[b]	coarse grains

[a]Product specification.
[b]Below the detection limit (~1 m^2/g).

The above measurements were all performed at ambient pressure. To investigate possible structural changes of fumed silica under pressure, we further measured *in situ* infrared absorption spectra up to ~6 GPa with a diamond anvil cell. KBr powders were used as both an infrared window and a pressure medium. The sample was confined in a small chamber, which was made by drilling a hole (100 μm in diameter) on a metal gasket (180 μm in thickness), in such a way that the silica fine particles were put on the top of the KBr powders, forming two layers consisting of fumed silica and KBr. The sample was then compressed between the diamond anvils with 300-μm culets together with ruby balls dispersed in the sample powders as pressure indicator. The pressure was determined by the Ruby fluorescence method.[27] For the present *in situ* infrared absorption measurements, we employed the fumed silica sample preheated at 1000 °C for 2 h.

III. RESULTS

A. Changes in the particle morphology with temperature

Table I shows the BET specific surface areas (S) of the as-received and heat-treated fumed silicas. We see that the surface area changes from ~400 to ~190 (~120) m^2/g when the samples is heated at 1000 (1100) °C. This decrease in surface area most likely results from sintering since it has been proposed that for fumed silicas the onset temperature of

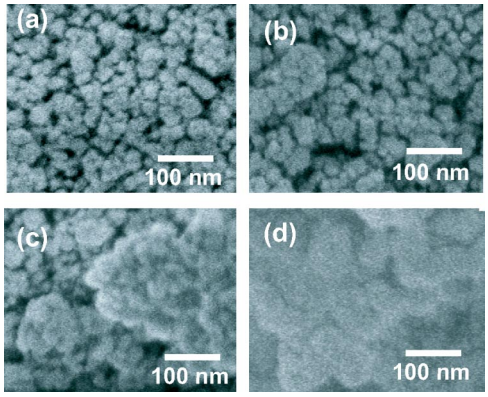

FIG. 1. FESEM images of fumed silica after heat treatment at (a) 900, (b) 1000, (c) 1100, and (d) 1200 °C for 2 h.

sintering is ~850 °C regardless of particle characteristics or heating times.[28] If we assume that each fumed silica particle is ideally spherical, we can estimate average diameter (d) of primary particles using a relationship $d=6.0\times10^3/(\rho S)$ where ρ is the specific density of primary particles of fumed silica (2.2 g/cm^3), S in m^2/g, and d in nm. According to this relationship, d is estimated to be 13 and 24 nm at 1000 and 1100 °C, respectively. Considering that d of the as received sample is 7 nm, we suggest that two or three particles approach one another and induce sintering or consolidation to form slightly larger primary particles in the temperature range 1000–1100 °C. FESEM observations also reveal the development of particle size with temperature (see Fig. 1). We should note, however, that the fumed silica samples heated at 1100 °C still retain the morphology of the original nanometer-sized silica particles. It is probable that the present sintering process does not occur by melting since melting of silica would require temperatures in excess of 2000 °C, implying that the present consolidation is induced by viscous sintering.

We have found that S decreases to the detection limit (~1 m^2/g) of the present volumetric adsorption apparatus at 1200 °C, which is near the glass transition temperature of silica glass.[29] This indicates that fine primary particles coalesce into bulklike silica at 1200 °C. Indeed, the sintered material heated at 1200 °C was not aggregates of nanometer-sized fine powders, as elucidated by the FESEM image shown in Fig. 1(d), but a collection of relatively large (~0.5 mm) grains.

B. Infrared absorption spectra

Figure 2 shows FTIR spectra of heat-treated fumed silicas as a function of the temperature of dehydroxylation along with an FTIR absorption spectrum of bulk silica glass. In agreement with the previous experiments, the infrared spectrum of bulk silica glass exhibits three main absorption bands at ~1100, ~800, and ~480 cm^{-1}, which are assigned to asymmetric stretching, symmetric stretching and bending motions of the Si—O—Si bonds, respectively.[30,31] The FTIR spectrum of fumed silica heated at 1200 °C is almost comparable to that of the bulk silica glass. This indicates that sintering is almost completed at 1200 °C to form coalescent bulklike materials, in accordance with the results mentioned in Sec. III A.

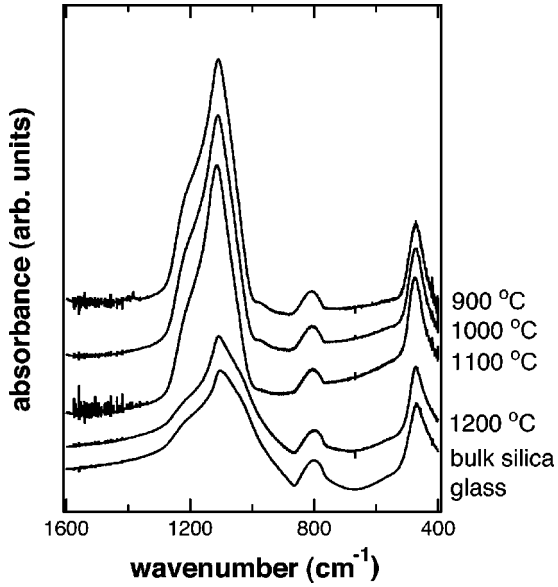

FIG. 2. Fourier transform infrared (FTIR) absorption spectra of fumed silica after heat treatment between 900 and 1200 °C. An additional weak shoulder at ~980 cm^{-1} is attributed to the bending vibration of residual Si—OH groups (Ref. 46). FTIR spectrum of normal bulk silica glass is also shown.

It should be noted, however, that FTIR spectra of fumed silica samples heated below 1100 °C have different spectral features than the one heated at 1200 °C or that of bulk silica glass. One of the striking differences can be seen in the Si—O—Si asymmetric stretching band at ~1100 cm^{-1}; in the FTIR spectra of fumed silica heated at 900–1100 °C this band has rather a narrow feature as compared with the corresponding band of bulk silica glass. In addition, the Si—O—Si symmetric stretching band at ~800 cm^{-1} observed for fumed silica samples heated at 900–1100 °C is located slightly at higher frequencies (808 cm^{-1}) than that of the bulk (800 cm^{-1}). These results suggest that the structure of dehydroxylated fumed silica is not identical to the structure of bulk silica glass; that is, the size dependence is seen in the structure of silica glass.

Figure 3 shows the infrared absorption spectra of an overtone mode of the Si—O—Si stretching band for the heat-treated fumed silica samples. We see from Fig. 3 that the peak position of this overtone mode shifts to higher frequencies with increasing heat-treated temperature. According to the empirical relationship between the peak position of the overtone mode ν and the fictive temperature T_f of silica glass[20]

$$\nu=2228.64+(43809.21/T_f) \quad (1)$$

we estimated the fictive temperature of the present fumed silica samples (see Table II). We see from Table II that the fictive temperature of the fumed silica decreases with increasing heating temperature. We should note, however, that the values of fictive temperature for the samples heated at

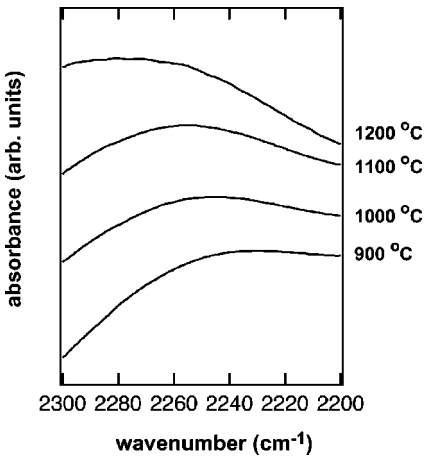

FIG. 3. Fourier transform infrared absorption spectra around 2260 cm^{-1} in the heat-treated silica samples. The peak originates from an overtone of the Si—O—Si stretching vibration at ~1100 cm^{-1}.

900–1100 and 1200 °C are rather high and low, respectively. This is probably because the linear relationship between ν and $1/T_f$ shown in Eq. (1) can be applied only to the frequency range from ~2255 to ~2263 cm^{-1} (Ref. 32); that is, the fictive temperature estimated for the present samples may not be quantitatively correct. A detailed structural analysis of fumed silica accompanied by the changes in the fictive temperatures will be given in a later section.

In situ infrared absorption spectra of fumed silica measured with the diamond anvil cell under high pressure are shown in Fig. 4(a). We see from Fig. 4(a) that the main Si—O—Si asymmetric stretching band becomes broad especially on the lower-frequency side of the band with increasing pressure. Thus, it is likely that fumed silica can accommodate applied pressure by changing the Si—O—Si bonding configurations, suggesting a highly deformable nature of the Si—O—Si linkages in the nanometer-sized silica particles. We also measured *in situ* infrared spectra of a normal bulk silica glass under the same condition as that employed for fumed silica [see Fig. 4(b)]. However, such a broadening of the main Si—O—Si stretching band as seen in the spectra of fumed silica was not observed, but the spectral feature was basically unchanged up to ~6 GPa. These results suggest that the random network of bulk silica is more rigid than that of fumed silica against applied pressure.

TABLE II. Estimation of fictive temperature from the peak position of the infrared absorption band at ~2260 cm^{-1} for heat-treated fumed silica samples. Equation (1) was used to estimate the fictive temperature.

heating temperature (°C)	peak position (cm^{-1})	fictive temperature (K)
900	2238.0	4680
1000	2247.5	2323
1100	2255.0	1661
1200	2269.0	1085

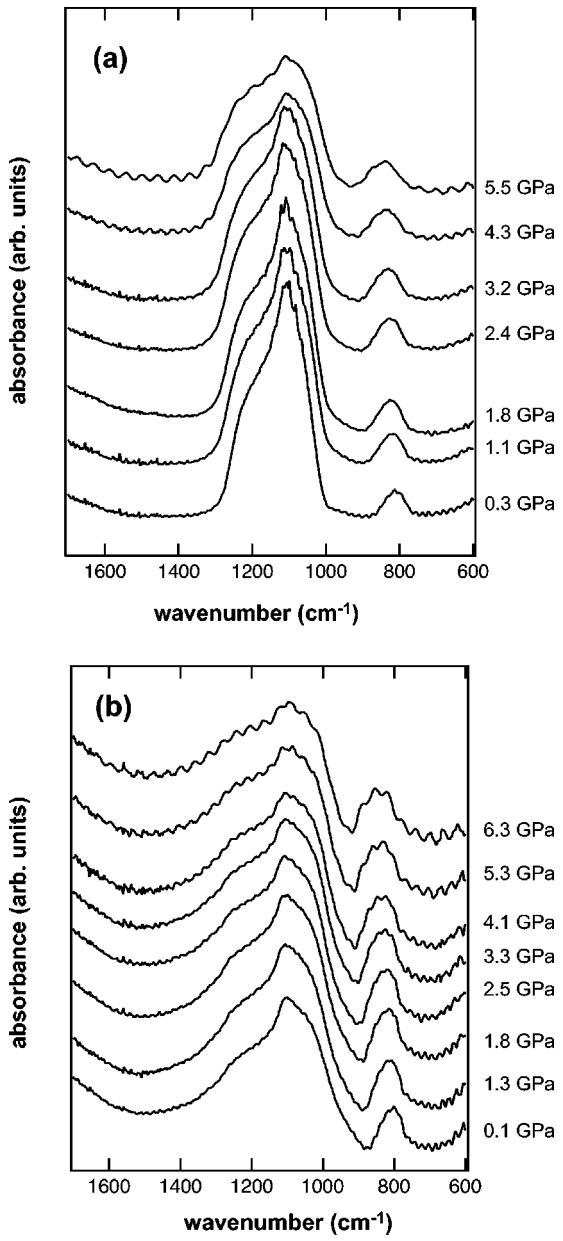

FIG. 4. *In situ* Fourier transform infrared absorption spectra of (a) compressed fumed silica and (b) compressed bulk silica glass under pressure. The effect of multiple reflections within the sample is seen as interference-fringe in each spectrum. The frequency region below ~600 cm^{-1} was not recorded because of the limitation of the MCT detector.

In other words, the structure of fumed silica will be rather flexible, allowing deformations of the Si—O—Si bonding configurations under high pressure.

C. Raman spectra

FT-Raman spectra of heat-treated fumed silicas along with bulk silica glass are shown in Fig. 5. Raman spectra of bulk silica glass have been investigated by a number of researchers.[33–35] It has been found that Raman spectra of silica glass have two sharp bands at 495 and 606 cm^{-1}, along with a dominant broad band (450 cm^{-1}) associated with the

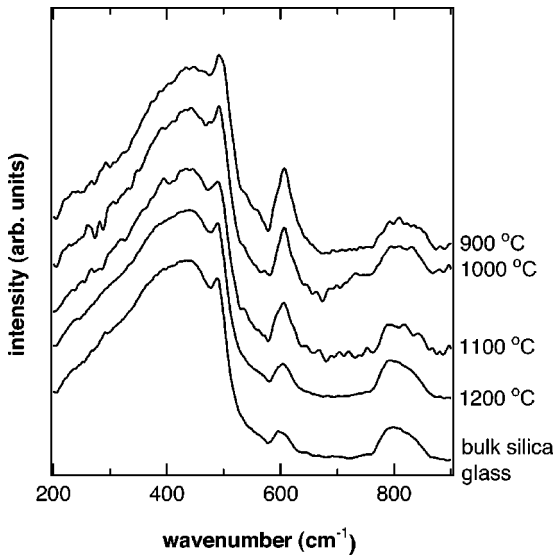

FIG. 5. Fourier transform Raman (FT-Raman) spectra of fumed silica after heat treatments between 900 and 1200 °C. FT-Raman spectrum of normal bulk silica glass is also shown.

bending motions of oxygen atoms in the random network. These two sharp bands at 495 and 606 cm^{-1} are referred to as D_1 and D_2, respectively, and are attributed to symmetric oxygen ring breathing vibrations of regular four-membered (D_1) and three-membered (D_2) silica rings.[36–38] As shown in Fig. 5, the D_1 and D_2 bands can be seen in the FT-Raman spectra of the heat-treated fumed silica samples as well. It is clear that the intensities of the D_1 and D_2 bands are rather high for the sample heated at 900 °C and tend to decrease with increasing temperature. When the temperature reaches 1200 °C, the FT-Raman spectrum of the heat-treated fumed silica becomes closely analogous to that of bulk silica glass, in agreement with the measurements of surface areas, FESEM, and infrared spectra mentioned earlier. It is hence quite likely that the concentrations of the D_1- and D_2-related structural units, or four-membered and three-membered silica rings, respectively, are dependent on the size of the primary particles. That is, in nanometer-sized silica particles the population of small-membered rings is larger than the one in the bulk. These ''regular'' rings are transformed into larger ''disordered'' rings with increasing temperature, leading to the atomic configurations similar to those in the bulk structure.

Previous Raman studies of silica glass versus T_f have demonstrated that the intensities of the D_1 and D_2 bands decreases with decreasing T_f.[22] This result is also in qualitatively agreement with the temperature dependence of T_f obtained from FTIR measurements shown in Table II.

D. X-ray diffraction measurements

The total Faber-Ziman structure factors[39] $S(Q)$, for the bulk silica glass and the heat-treated fumed silica samples are shown in Fig. 6. As far as the $S(Q)$ data are concerned, we do not see any noticeable difference between the heat-treated fumed silica and the bulk silica glass except for the Q range below $\sim$0.5 Å^{-1}. An abrupt increase seen in $S(Q)$ of heat-treated fumed silicas probably results from the structural fluctuation or the aggregated structure formed from the nanometer-sized primary particles.[13] To get the information in real space, we calculate total correlation functions, $T(r)$, (see Fig. 7) from the weighted interference functions

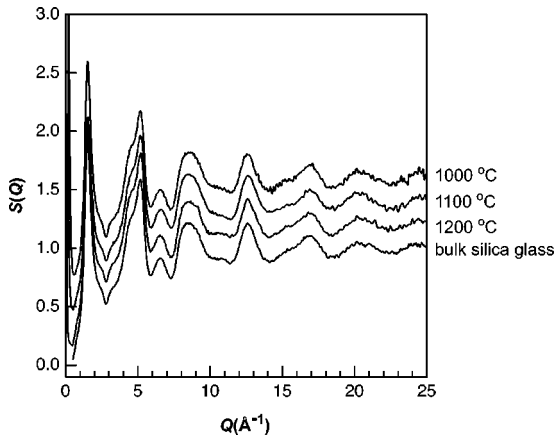

FIG. 6. The x-ray structure factors $S(Q)$ of normal bulk silica glass and heat-treated fumed silica. Successive curves are displaced upward by 1 for clarity.

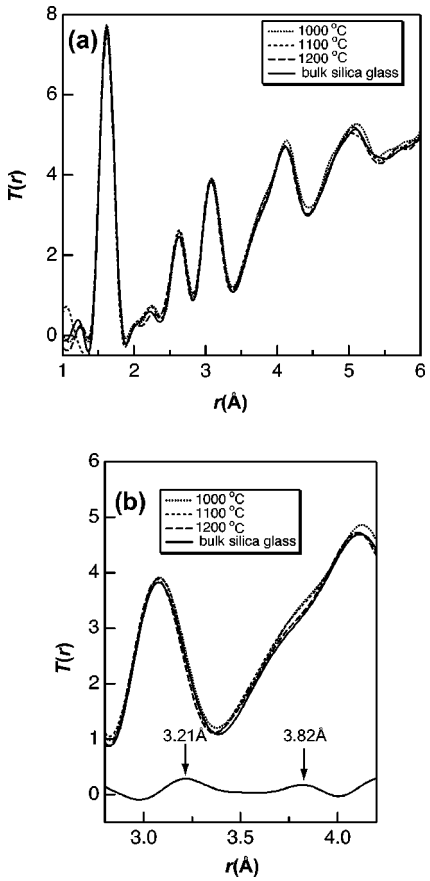

FIG. 7. (a) Total correlation functions $T(r)$ of normal bulk silica glass and heat-treated fumed silica. (b) Expand plot of $T(r)$ in the distance region from 2.8 to 4.2 Å. The curve shown in the bottom is obtained by subtracting $T(r)$ at 1000 °C from the one at 1200 °C.

$Q[S(Q)-1]$ by Fourier transformation up to $Q_{max}=25$ Å^{-1},

$$T(r)=4\pi\rho r+\frac{2}{\pi}\int_{Q_{min}}^{Q_{max}}M(Q)Q[S(Q)-1]\sin(Qr)dQ, \tag{2}$$

where ρ is the total number density and $M(Q)$ is a Lorch modification function[40] to reduce termination effects arising from the finite upper limit of Q. As in the case of the $S(Q)$ data, the $T(r)$ functions of the heat-treated fumed silicas appear to be similar to that of the bulk silica glass. However, when we have a close look at the distance region especially from 2.5 to 4 Å, there exist slight but appreciable differences among the present $T(r)$ functions. That is, the first-neighbor O—O (~2.6 Å) and Si—Si (~3.1 Å) peaks in $T(r)$ of the fumed silicas heated at 1000 or 1100 °C are higher than those of the corresponding peaks observed for the one heated at 1200 °C. On the other hand, the $T(r)$ function of the heat-treated fumed silica at 1200 °C is virtually identical to that of the bulk silica glass, in harmony with the other experiments such as specific surface areas and vibrational spectroscopies. Considering that these peaks arise from the intratetrahedral (O—O) and intertetrahedral (Si—Si) interactions of the SiO_4 units in the silica network, we suggest that, in small silica particles, the SiO_4 tetrahedral units along with their first-neighbor connectivity has a peculiar structural feature that is basically different from the one in the bulk. It is hence quite likely that as the size of primary particles grows during sintering, the structure and connectivity of the constituent SiO_4 tetrahedra will be altered, leading to such a random network structure as seen in the bulk phase.

IV. DISCUSSION

Thus, we have shown that the structure of fumed silica is different from that of the bulk silica glass in terms of infrared and Raman spectra and x-ray diffraction data. It is natural to assume that this difference stems form the surface structure of each primary particle of fumed silica. According to previous MD simulations,[15,16] nanometer-sized silica clusters can be represented by a shell like structure. That is, the structure and density of the cluster surface are substantially different from those of the interior of the cluster, and the ''surface shell'' has the same thickness and width regardless of size. The width of the surface is estimated to be ~2 Å,[15,16] which corresponds to the distance of one or two Si—O bonds. It has also been suggested that the interior of the cluster is structurally equivalent to the bulk.[15]

However, the present infrared measurements of fumed silica are not totally consistent with the results of these MD simulations on silica clusters. If the structure of the interior of silica fine particles is equivalent to the bulk and the structural difference can only be seen at the surface, the resulting infrared spectra of the particles will have a spectral feature similar to the bulk, and a possible additional feature relevant to the surface will be superimposed on the spectrum. In contrast to the expectation, the FTIR spectra of the unconsolidated fumed silica samples have a spectral feature that is basically different from that of the bulk. As mentioned previously, the ~1100-cm^{-1} band of the fumed silica heated at 900–1100 °C is rather narrow as compared with the corresponding band of the bulk one (see Fig. 2). The ~1100-cm^{-1} band of the bulk has a shoulder at ~1000 cm^{-1} on the lower frequency side of the band, extending to the higher-frequency tail of the ~800-cm^{-1} band. In the FTIR spectra of the unconsolidated fumed silica, however, we do not recognize such a shoulder at ~1000 cm^{-1}, and the infrared absorption is virtually missing in the frequency region from 880 to 990 cm^{-1}. This indicates that not only at the surface but also in the interior of fumed silica, the distribution of the Si—O—Si bonding environments or, strictly speaking, the distribution of the force constants and the reduced masses associated with the Si—O—Si asymmetric stretching vibrations at ~1100 cm^{-1}, is different from that of the bulk silica glass.

According to the FT-Raman spectra shown in Fig. 5, such a structural difference between fumed and bulk silicas may arise from a difference in the distribution of the size of the ''rings'' in the network. The intensities of the D_1 and D_2 peaks in the FT-Raman spectra of unconsolidated fumed silica are higher than those of the consolidated fumed silica or the bulk silica, implying that regular three- and four-membered rings are more abundant in silica fine particles than in the bulk.

The signature of the three- and four-membered rings in fumed silica can be found in the present x-ray diffraction data as well. In the three- and four-membered rings, the second-neighbor Si—O separations give rise to characteristic distances at ~3.2 and ~3.8 Å, respectively, because of their regular geometries, as seen in the results of ab initio molecular orbital calculations using a silica-based cluster of atoms (see Fig. 8). Indeed, $T(r)$ of the fumed silica samples heated at 1000 and 1100 °C have additional features in the corresponding distance regions as compared with $T(r)$ of the bulk silica glass. This can be highlighted when we take a difference between $T(r)$s of the heat-treated fumed silica samples heated at 1000 and 1200 °C [see Fig. 7(b)]. It is clear from Fig. 7(b) that there exist two peaks at ~3.2 and ~3.8 Å in the difference total correlation function, corresponding to the second-neighbor Si—O separations peculiar to the three- and four-membered rings, respectively.

The present experimental results further demonstrate that the population of the n-membered rings ($n=3,4$) becomes lower with increasing temperature; the structure of the sample heated at 1200 °C is almost equivalent to the bulk. The observed phenomena can be interpreted as follows. The existence of the small-membered rings in the bulk will impose additional structural constraints on the atomic configurations around the rings because of their regular or rigid geometries. It is hence reasonable to assume that such small n-membered rings ($n=3,4$) cannot exist as is during the sintering process. That is, in the event of consolidation, these regular small-membered rings will be reorganized into larger ones to form the bulk phase, otherwise the rigidity of small-membered rings will cause unfavorable strain energies in the random SiO_2 network.

Finally, we give a brief explanation as to why fumed silica

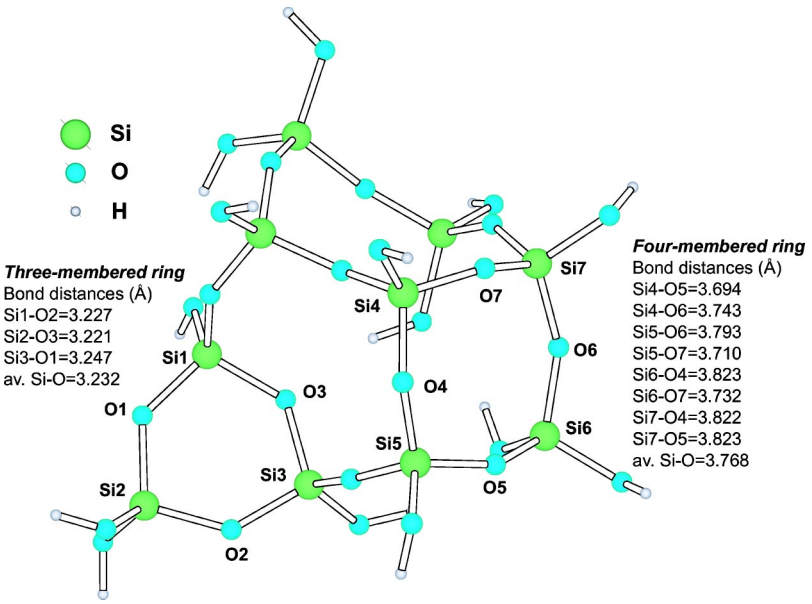

FIG. 8. A cluster of atoms modeling the local structure of three-and four-membered rings in the SiO_2 network. The surface oxygen atoms in the cluster are terminated by hydrogen atoms to eliminate the dangling bonds. The geometry of the cluster was fully optimized at the Hartree-Fock level using the 6-31G(d) basis set (Ref. 47).

can accommodate a large number of regular small-membered rings as compared with the bulk. As mentioned in the Introduction, fumed silica is synthesized with $SiCl_4$ in the oxygen/hydrogen flame at 1400–1800 °C. It is quite likely that free isolated Si_nO_m clusters are originally formed in the early stage of the hydrothermal process, leading to highly viscous droplets of amorphous silicon dioxide having the particle sizes of ~10–~20 nm.[41] Previous theoretical calculations on small silica clusters have demonstrated that free isolated $(SiO_2)_n$ clusters ($\sim 5 \leqslant n \leqslant \sim 20$) tend to form atomic configurations consisting of small-membered rings such as two-, three-, and/or four-membered rings.[42–45] In other words, these small-membered rings are energetically favored in such small isolated clusters, forming rather regular symmetric structures. When these isolated clusters are fused together to build up nanometer-sized primary particles, the original atomic configurations of the clusters will be reorganized to form a stable random network consisting mostly of larger *n*-membered rings ($n=5-7$). However, as shown in the *in situ* infrared measurements of fumed silica under high pressure (see Fig. 4), the Si—O—Si network of fumed silica will be more flexible than that of the bulk and, therefore, some of the small-membered rings will survive even in the nanometer-sized particles. That is, in fumed silica particles, the structural constraints derived from the small-membered rings can be, although partly, compensated by the atomic rearrangements of the surrounding network, reducing the strain energies of the resultant primary particles. Thus, as far as the ring structure is concerned, it can be said that fumed silica has a ''memory'' of the small isolated clusters formed originally at very high temperatures, explaining a high T_F for the unconsolidated samples shown in Table II. As the size of the particles increases during the sintering process, however, such atomic rearrangements will induce subsequent strains in the other parts of the network. To reduce these strains, cooperative structural reorganizations will eventually occur throughout the network to form the bulklike structure. These structural reorganizations leading to the bulklike structure will account for a observed decrease in T_f for the sample heated at 1200 °C.

V. CONCLUSIONS

We have demonstrated that the structure of nanometer-sized particles of fumed silica is not identical to that of the bulk. The FT-Raman spectra of fumed silica indicate that the population of thee- and four-membered rings is higher in fumed silica than in the bulk. These small-membered rings in fumed silica still survive even after heating the samples up to 1100 °C. At 1200 °C, which is near the glass transition temperature of silica glass, respective primary particles coalesce into a large mass of silica grains, leading to the structure almost identical to the one in the normal bulk silica glass. This indicates that these silica fine particles can be sintered at temperatures far below the melting point (~2000 °C), and viscous sintering plays a vital role in inducing the present consolidation process, accompanied by the transformation of the ring size distribution from smaller to larger ones. It has also been elucidated from *in situ* infrared absorption measurements under high pressure that the Si—O—Si network of fumed silica is more flexible than that of the bulk. Such a flexible nature of the Si—O—Si network in nanometer-sized particles will give a clue to understand the reason why fumed silica can accommodate a large number of small-membered silica rings as compared with the bulk silica glass.

ACKNOWLEDGMENTS

The synchrotron radiation experiments were performed at the SPring-8 with the approval of the Japan Synchrotron Radiation Research Institute (Proposal No. 2002B0375-ND1-np). We are grateful to Professor N. Yoshida and H. Nakata (Kobe University) for the measurements of specific surface area of the samples. We also thank Professor K. Nakanishi and H. Saito (Kyoto University) for carrying out FESEM experiments.

[1] S. H. Tolbert and A. P. Alivisatos, Science **265**, 373 (1994).
[2] V. R. Palkar, P. Ayyub, S. Chattopadhyay, and M. Multani, Phys. Rev. B **53**, 2167 (1996).
[3] Z. Wang, S. K. Saxena, V. Pischedda, H. P. Liermann, and C. S. Zha, Phys. Rev. B **64**, 012102 (2001).
[4] J. S. Altman, D. Lee, J. D. Chung, J. Song, and M. Choi, Phys. Rev. B **63**, 161402 (2001).
[5] Y. D. Glinka, S.-H. Lin, and Y.-T. Chen, Phys. Rev. B **62**, 4733 (2000).
[6] V. V. Afanas'ev and A. Stesmans, Phys. Rev. B **59**, 2025 (1999).
[7] D. P. Yu, Q. L. Hang, Y. Ding, H. Z. Zhang, Z. G. Bai, J. J. Wang, Y. H. Zou, W. Qian, G. C. Xiong, and S. Q. Feng, Appl. Phys. Lett. **73**, 3076 (1998).
[8] C. C. Liu and G. E. Maciel, J. Am. Chem. Soc. **118**, 5103 (1996), and references therein.
[9] B. A. Morrow and I. A. Cody, J. Phys. Chem. **80**, 1995 (1976).
[10] B. C. Bunker, D. M. Haaland, T. A. Michalske, and W. L. Smith, Surf. Sci. **222**, 95 (1989).
[11] T. Freltoft, J. K. Kjems, and S. K. Shinha, Phys. Rev. B **33**, 269 (1986).
[12] A. J. Hurd, D. W. Schaefer, and J. E. Martin, Phys. Rev. A **35**, 2361 (1987).
[13] J. H. Page, W. J. L. Buyers, G. Dolling, P. Gerlach, and J. P. Harrison, Phys. Rev. B **39**, 6180 (1989).
[14] T. Campbell, R. K. Kalia, A. Nakano, F. Shimojo, K. Tsuruta, P. Vashishta, and S. Ogata, Phys. Rev. Lett. **82**, 4018 (1999).
[15] A. Roder, W. Kob, and K. Binder, J. Chem. Phys. **114**, 7602 (2001).
[16] I. V. Schweigert, K. E. J. Lehtinen, M. J. Carrier, and M. R. Zachariah, Phys. Rev. B **65**, 235410 (2001).
[17] T. Uchino, A. Sakoh, M. Azuma, M. Takano, M. Takahashi, and T. Yoko, J. Phys.: Condens. Matter **14**, 11111 (2002).
[18] T. Uchino, A. Sakoh, M. Azuma, S. Kohara, M. Takahashi, M. Takano, and T. Yoko, Phys. Rev. B **67**, 092202 (2003).
[19] M. L. Hair, J. Non-Cryst. Solids **19**, 299 (1975).
[20] A. Agrawal, K. M. Davis, and M. Tomozawa, J. Non-Cryst. Solids **185**, 191 (1995).
[21] A. Q. Tool, J. Am. Ceram. Soc. **29**, 240 (1946).
[22] A. E. Geissberger and F. L. Galeener, Phys. Rev. B **28**, 3266 (1983).
[23] G. J. Young, J. Colloid Sci. **13**, 67 (1958).
[24] H. F. Poulsen, J. Neuefeind, H.-B. Neumann, J. R. Schneider, and M. D. Zeidler, J. Non-Cryst. Solids **188**, 63 (1995); J. Neuefeind and H. F. Poulsen, Phys. Scr. **T57**, 112 (1995).
[25] M. Isshiki, Y. Ohishi, S. Goto, K. Takeshita, and I. Ishikawa, Nucl. Instrum. Methods Phys. Res. A **467–468**, 663 (2001).
[26] S. Kohara, K. Suzuya, Y. Kashihara, N. Matsumoto, N. Umesaki, and I. Sakai, Nucl. Instrum. Methods Phys. Res. A **467–468**, 1030 (2001).
[27] H. K. Mao, J. Xu, and P. M. Bell, J. Geophys. Res. **91**, 4673 (1986).
[28] G. J. Young, J. Colloid Sci. **13**, 67 (1958).
[29] J. D. Mackenzie, J. Am. Ceram. Soc. **47**, 76 (1964).
[30] E. R. Lippincott, A. V. Valkenburg, C. E. Weir, and E. N. Bunting, J. Res. Natl. Bur. Stand. **61**, 61 (1958).
[31] R. Hanna, J. Am. Ceram. Soc. **48**, 595 (1965).
[32] H. Kakiuchida, K. Saito, and A. J. Ikushima, J. Appl. Phys. **93**, 777 (2003).
[33] P. McMillan, Am. Mineral. **69**, 622 (1984).
[34] M. Hass, J. Phys. Chem. Solids **31**, 415 (1970).
[35] G. E. Walrafen, T. C. Chu, and M. S. Hokmabadi, J. Phys. Chem. **94**, 5658 (1990).
[36] F. L. Galeener, Solid State Commun. **44**, 1037 (1982).
[37] A. Pasquarello and R. Car, Phys. Rev. Lett. **80**, 5145 (1998).
[38] T. Uchino, Y. Tokuda, and T. Yoko, Phys. Rev. B **58**, 5322 (1998).
[39] T. E. Faber and J. M. Ziman, Philos. Mag. **11**, 153 (1965).
[40] E. A. Lorch, J. Phys. C **2**, 229 (1969).
[41] H. Barthel, M. Heinemann, M. Stintz, and B. Wessely, Part. Part. Syst. Charact. **16**, 169 (1999).
[42] J. A. W. Harkless, D. K. Stillinger, and F. H. Stillinger, J. Phys. Chem. **100**, 1098 (1996).
[43] C. Xu, W. Wang, W. Zhang, J. Zhang, L. Liu, Q. Kong, L. Zhao, Y. Long, K. Fan, S. Qian, and Y. Li, J. Phys. Chem. A **104**, 9518 (2000).
[44] S. K. Nayak, B. K. Rao, S. N. Khanna, and P. Jena, J. Chem. Phys. **109**, 1245 (1998).
[45] L.-S. Wang, J. B. Nicholas, M. Dupuis, H. Wu, and S. D. Colson, Phys. Rev. Lett. **78**, 4450 (1997).
[46] A. Burneau and J.-P. Gallas, in *The Surface Properties of Silicas*, edited by A. P. Legarand (Wiley, Chichester, 1998), pp. 147–234.
[47] M. S. Gordon, Chem. Phys. Lett. **76**, 163 (1980), and references therein.